Materials Science & Engineering C 89 (2018) 307–315

Contents lists available at ScienceDirect

Materials Science & Engineering C

journal homepage: www.elsevier.com/locate/msec

Cyclodextrin- and dendrimer-conjugated graphene oxide as a nanocarrier for the delivery of selected chemotherapeutic and photosensitizing agents

Ampornphan Siriviriyanun[a], Ya-Ju Tsai[b], Siew Hui Voon[c], Siaw Fui Kiew[d], Toyoko Imae[a,b,*], Lik Voon Kiew[c], Chung Yeng Looi[c], Won Fen Wong[e], Hong Boon Lee[d], Lip Yong Chung[d,**]

[a] Graduate Institute of Applied Science and Technology, National Taiwan University of Science and Technology, 43 Section 4, Keelung Road, Taipei 10607, Taiwan, ROC
[b] Department of Chemical Engineering, National Taiwan University of Science and Technology, 43 Section 4, Keelung Road, Taipei 10607, Taiwan, ROC
[c] Department of Pharmacology, Faculty of Medicine, University of Malaya, 50603 Kuala Lumpur, Malaysia
[d] Department of Pharmacy, Faculty of Medicine, University of Malaya, 50603 Kuala Lumpur, Malaysia
[e] Department of Medical Microbiology, Faculty of Medicine, University of Malaya, 50603 Kuala Lumpur, Malaysia

ARTICLE INFO

Keywords:
Graphene oxide
Cyclodextrin
Dendrimer
Photosensitizer
Drug delivery
Nanoparticle

ABSTRACT

In this study, nanohybrid materials consisting of graphene oxide (GO), β-cyclodextrin (CD) and poly(amido amine) dendrimer (DEN) were successfully prepared by covalent bonding. GO-CD and GO-CD-DEN were found to be potential nanocarriers for anticancer drugs including chemotherapeutics (doxorubicin (DOX), camptothecin (CPT)) and photosensitizer (protoporphyrin IX (PpIX)). GO-CD possessed 1.2 times higher DOX-loading capacity than GO due to inclusion of additional DOX to the CD. The drug loading on GO-CD-DEN increased in the order: DOX < PpIX < CPT. Enhanced cytotoxicity of DOX and CPT and also the photocytotoxicity of PpIX were observed when the drugs were loaded in GO-CD and GO-CD-DEN. Functionalization of GO with CD and CD-DEN increased the uptake in cancer cells, and both GO-CD and GO-CD-DEN nanohybrids remained in the cytoplasm and were not uptaken into the nucleus, as shown in the flow cytometry and high-content screening study.

1. Introduction

Carbon-based nanocarriers such as carbon nanotube [1–3], carbon nanohorn [4,5], and graphene oxide (GO) [6–8] have been explored as drug delivery system [9–14]. Among them, GO is considered as a promising nanocarrier over other carbon materials due to its two-dimensional structure that provides high specific surface area [15] for high drug loading capacity [16,17]. Large amount of drugs can be loaded onto both side of graphene sheet through π–π stacking interaction, covalent bonding or electrostatic interaction [6–8]. The amphiphilic nature of GO nanocarriers may also improve the solubility of anticancer drugs in aqueous environment [18].

GO nanocarriers have been functionalized with surface coatings such as polymers to improve their biocompatibility [19] and targeting molecules for active targeting [6–8,17]. In this study, we explore the use of cyclodextrins (CDs) and poly(amido amine) (PAMAM) dendrimers as the surface coatings of GO. CDs are cyclic oligosaccharides comprised of α-1,4-linked glucopyranose units with a hydrophilic exterior surface and a hydrophobic cavity [20,21]. Among the three naturally-occurring CDs – α-, β- and γ-CD [22–25], β-CD is widely used in drug delivery because the cavity of its torus shape is suitable to form inclusion complex with both hydrophilic and hydrophobic drug molecules, particularly, with anthracycline drugs including doxorubicin (DOX) [22,26–31]. Additionally, CD is able to prevent self-association of DOX in aqueous medium that could diminish its antitumor activity [32]. Thus, the functionalization of GO with CD is expected to improve the water dispersibility [33] and drug loading of GO.

We also conjugated GO nanocarrier with PAMAM dendrimers to further improve cellular uptake of GO [34,35] as PAMAM dendrimers were reported to be electrostatically associated with lipid membranes and amphiphilic bilayers and hence, promoting cellular uptake [36,37]. Previously, we had demonstrated that the GO conjugate with dendrimer showed high drug loading and release efficiencies for DOX, and efficiently taken up by HeLa cells [38]. In the present work, anticancer drugs such as chemotherapeutics (DOX and camptothecin) and a photosensitizer (protoporphyrin IX) were respectively loaded onto the β-CD-conjugated GO (GO-CD) and β-CD- and dendrimer-conjugated GO (GO-CD-DEN). The respective GO-CD/drug and GO-CD-DEN/drug assemblies were characterized, and tested in vitro for anticancer efficacy, based on the assumption that the drug loading of GO occurs via

* Correspondence to: T. Imae, Graduate Institute of Applied Science and Technology, National Taiwan University of Science and Technology, 43 Section 4, Keelung Road, Taipei 10607, Taiwan, ROC.
** Correspondence to: L.Y. Chung, Department of Pharmacy, Faculty of Medicine, University of Malaya, 50603 Kuala Lumpur, Malaysia.
E-mail addresses: imae@mail.ntust.edu.tw (T. Imae), chungly@um.edu.my (L.Y. Chung).

https://doi.org/10.1016/j.msec.2018.04.020
Received 28 July 2017; Received in revised form 13 September 2017; Accepted 10 April 2018
Available online 12 April 2018
0928-4931/

adsorption onto the graphene sheet and as inclusion to CD. The drugs loaded onto the current nanohybrids are expected to exhibit higher cellular uptake, better drug activity, such as killing cancer cells more efficiently than free drugs itself [39]. Thus, the present work provides new GO-based nanocarrier materials that could be exploited as potential drug nanocarriers for cancer therapy.

2. Materials and methods

2.1. Materials and characterizations

An aqueous dispersion of GO (0.275 mg/cm^3) was purchased from UniRegion Bio-Tech, Taiwan. β-CD was purchased from Wako, Japan. *N*-hydroxysuccinimide (NHS), 1-[3-(dimethylamino)propyl]-3-ethylcarbodiimide hydrochloride (EDC), 4-dimethylaminopyridine (DMAP), *N,N′*-dicyclohexylcarbodiimide (DCC), dimethylformamide, ethylenediamine, and *p*-toluenesulfonyl chloride (*p*-TsCl) were purchased from ACROS, USA. OH-Terminated fourth generation PAMAM dendrimer, fluoresceinyl glycine amide (FGA), camptothecin (CPT) and protoporphyrin IX (PpIX) were purchased from Sigma-Aldrich, USA. HeLa cells and doxorubicin (DOX) were kindly donated by Prof. H. C. Tsai, National Taiwan University of Science and Technology, Taiwan. Other reagents were of commercial grade. Ultra-pure (Millipore Milli–Q) water with a resistivity of 18.2 MΩ·cm was used for all syntheses and measurements.

Dynamic light scattering (DLS) and zeta potential were measured on a nanoparticle analyzer (Horiba SZ-100) with a 532 nm laser. Infrared (IR) absorption spectra were recorded as KBr discs on an FT-IR spectrometer (Nicolet, Nexus 670). Ultra violet (UV)–visible absorption spectroscopic measurements were performed on a Jasco V–670 spectrometer with a 1 mm quartz cell. Fluorescence was measured with a Hitachi F–3010 fluorometer at a scan rate of 30 nm/min using a 10 mm quartz cell. Suspensions of sample powders in water under a sonication were prepared for measurements of UV–visible absorption and fluorescence spectra. Atomic force microscopic (AFM) observation was performed in air using a Digital Instruments NanoScope III apparatus (Veeco). The sample solutions were dropped directly onto the freshly-cleaved mica surface, and then dried in air.

2.2. Preparation of graphene oxide nanocarriers with β-cyclodextrin and OH-terminated PAMAM dendrimer

Aminated-β-CD (amino-β-CD) was prepared via two steps of tosylation and amination following the previously reported method [38]. Briefly, the suspension of β-CD (20 g) and *p*-TsCl (15 g) in an aqueous NaOH solution (0.4 M, 200 ml) was stirred for 2 h at 0 °C, and unreacted *p*-TsCl was filtered off. Crude tosylated-β-CD (tosyl-β-CD) was precipitated at pH 7 and recrystallized from hot water (90 °C, 200 ml). Tosyl-β-CD (1 g) dissolved in ethylenediamine (50 ml) was refluxed under stirring at 40 °C for 24 h. The unreacted ethylenediamine was evaporated to condense the solution. Crude amino-β-CD was precipitated from the condensed solution in acetone and dissolved in a mixture of methanol and water (3:1) to reprecipitate from acetone.

Size-controlled GO nanosheet was prepared by the mechanical cleavage of commercial GO using the ultrasonic processor [26]. The average hydrodynamic particle size of GO nanosheet was evaluated from DLS to be 100 nm, which was small compared to the commercial GO (550 nm). Nanocarrier material of GO-CD was prepared by using condensing agents (EDC and NHS) for amide formation between a carboxylic acid group on GO and an amine group on amino-β-CD [39] as shown in Scheme 1(a) according to the conventional amidation procedure [26,40]. Subsequently, the conjugation of dendrimer on GO-CD was performed by the esterification binding of carboxylic acid group on GO with OH-terminal groups on PAMAM dendrimer (Scheme 1(b)) following the previous procedure using condensation reagents (DCC and DMAP) [38]. Briefly, an aqueous dispersion (8 ml) of GO-CD was centrifuged, and the centrifugate was dispersed in dimethylformamide (4 ml). A dimethylformamide solution (4 ml) of GO-CD was mixed with a dimethylformamide solution (0.4 wt%, 6 ml, 90 μM) of the dendrimer, and the mixture was esterified by adding DCC and DMAP and maintaining for 24 h at room temperature. The product (GO-CD-DEN) was collected, rinsed and re-dispersed in water.

2.3. Loading and release of drugs on GO, GO-CD and GO-CD-DEN

DOX loading on GO, GO-CD and GO-CD-DEN was carried out as shown in Scheme 1(c). An aqueous dispersion (2 ml) of GO, GO-CD or GO-CD-DEN was mixed with DOX (2 ml) at different DOX concentrations of 0.1–2.0 mg/ml [26]. The mixture was sonicated, adjusted to pH 7 and then kept stirring overnight at room temperature for 24 h in the dark. Then, the dispersion was adjusted to pH 4 and centrifuged at 13,500 rpm for 1 h to remove unbound DOX from the DOX-loaded GO (GO/DOX), GO-CD (GO-CD/DOX) or GO-CD-DEN (GO-CD-DEN/DOX). The concentration of unbound DOX in the supernatant was determined quantitatively from absorbance at an absorption band of 233 or 500 nm. The amount of loaded DOX against nanocarrier (GO, GO-CD or GO-CD-DEN) was calculated by subtracting the amount of unbound DOX from the initial amount of DOX and divided with the amount of GO, GO-CD or GO-CD-DEN.

Controlled release of DOX was carried out in a phosphate buffered saline (PBS) at room temperature. A dispersion of GO/DOX, GO-CD/DOX or GO-CD-DEN/DOX in dialysis membrane tube with molecular weight cut-off (MWCO) = 6000–8000 was dialyzed under constant stirring in 30 ml of distilled water at pH 5.5 and 7.4, respectively. Then the amount of DOX released from DOX-loaded nanocarrier was quantified from absorbance of an absorption band at 233 nm of DOX outside the dialysis membrane tube at various time intervals. The amount of DOX released was averaged for triplicate measurements. The loading and release of CPT and PpIX on the nanocarriers were examined using the same procedures. The quantification of dugs was carried out at an absorption band at 243 nm for CPT and at 420 nm for PpIX.

2.4. In vitro cytotoxicity and photocytotoxicity assay of GO-based nanocarriers

HeLa cells (1×10^4 cells/ml) were grown in 200 μl of Dulbecco's modified Eagle's medium (DMEM, Gibco, Brazil) in a humidified incubator with 5% CO_2 at 37 °C. Thereafter, the cells were treated with nanocarriers and DOX-loaded nanocarriers at various concentrations. Cells were further incubated at 5% CO_2 and 37 °C for 72 h and the viability of cells was assessed using 3-(4,5-dimethylthiazol-2-yl)-2,5-diphenyl tetrazolium bromide (MTT) assay. Briefly, 10 μl of MTT (5 mg/ml in PBS) was added to each well and incubated for 3 h. The supernatant was removed, and 100 μl of dimethylsulfoxide was added to dissolve the purple formazan crystals. The optical density of each well was measured at 570 nm using a microplate reader. The viability of the cells in response to the treatment of GO nanohybrids was calculated as a cell viability (%) = (optical density treated / optical density control) × 100. Cell viability in the presence of a solvent control (PBS) was determined concurrently.

MDA-MB-231 and MCF-7 human breast cancer cells were grown and maintained in DMEM supplemented with 10% fetal bovine serum (FBS) and 1% penicillin-streptomycin at 37 °C in a 5% CO_2 humidified chamber. MDA-MB-231 cells were seeded into 96-well plates at 5000 cells/well and were incubated overnight to allow cells to adhere. MDA-MB-231 cells were treated with nanocarriers and DOX-loaded nanocarriers at various concentrations. The cells were then incubated for 24 h at 37 °C in 5% CO_2 before cell viability was assessed using the MTT assay. Following this, the cytotoxicity of DOX-, CPT- and PpIX-loaded nanocarriers were also evaluated in both MDA-MB-231 and MCF-7 human breast cancer cells.

To evaluate the photocytotoxicity of PpIX-loaded GO-CD and GO-

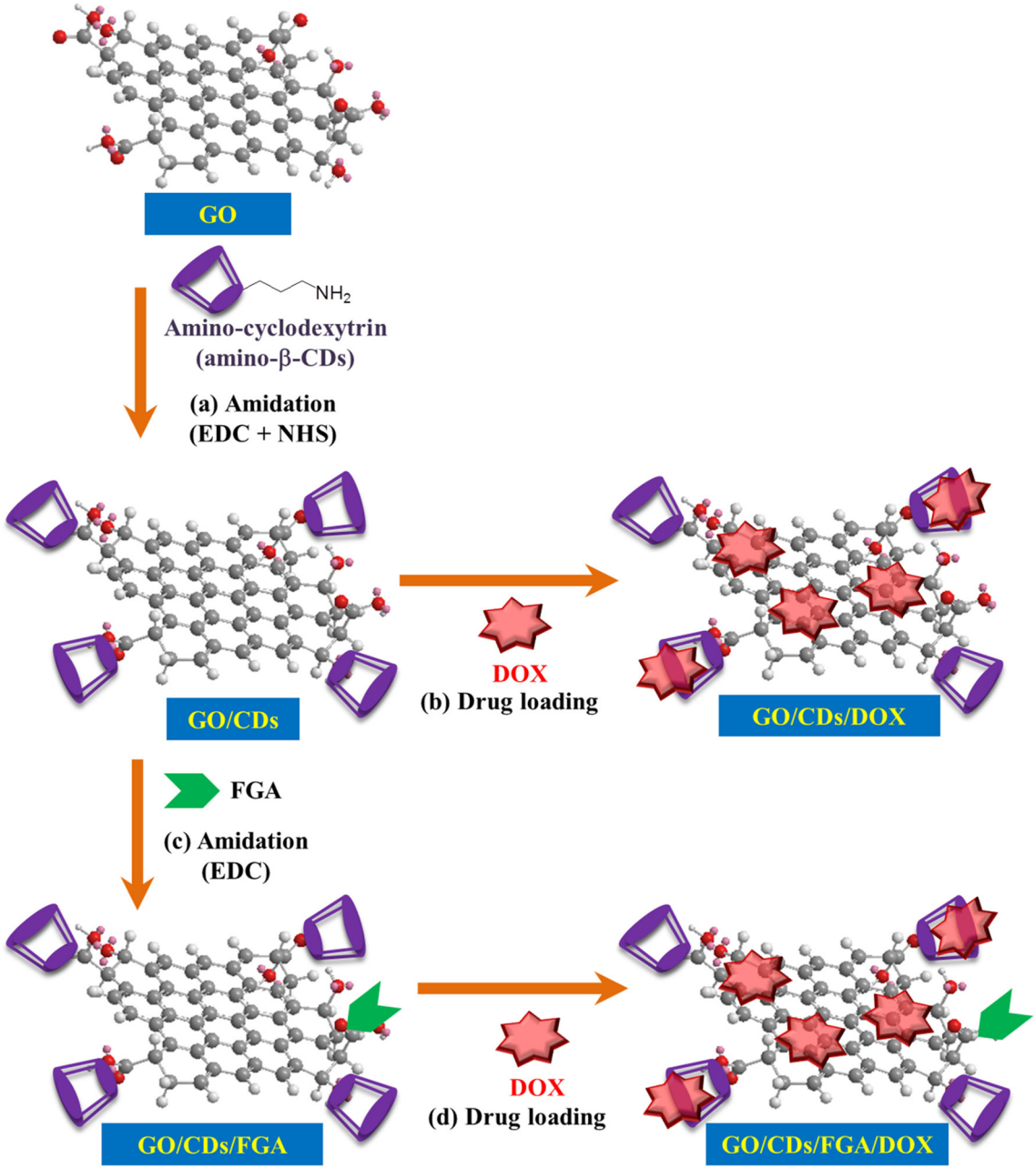

Scheme 1. Schematic Illustration of preparation of graphene oxide composites.

CD-DEN, MDA-MB-231 and MCF-7 cells treated with GO-nanohybrids were irradiated with 5.3 J cm^{-2} of light from a broad-spectrum halogen light source at a fluence rate of 8.9 mW cm^{-2} for 10 min. The cells were further incubated for 24 h before cell viability was assessed using the MTT assay. A set of dark control experiments in which the cells were not irradiated was concurrently set up and performed.

2.5. Cellular uptake of FGA-labeled GO nanocarriers by flow cytometry and high content screening

FGA (0.26 mM, 2 ml) was chemically bound to GO, GO-CD or GO-CD-DEN in an aqueous suspension (2 ml) by amidation reaction. Unbound FGA was removed by ultracentrifugation at 13,500 rpm for 1 h. The centrifugate (FGA-GO-CD or FGA-GO-CD-DEN) was rinsed three times with water and then redispersed in water. Then, the prepared FGA-GO-CD and FGA-GO-CD-DEN was stored at 4 °C until use. The amount of FGA conjugated on the nanocarriers was determined by estimating the FGA fluorescence emission intensity (area under curve, AUC) from 500 to 540 nm following excitation at 488 nm. One hundred microliters of FGA-labeled nanocarriers were added to the 96-well black plate (Corning, NY, USA) and the emission intensity was measured using a SpectraMax® M3 multi-mode microplate reader (Molecular Devices Sunnyvale, CA, USA). The AUC was calculated using ImageJ 1.49 (NIH, Bethesda, MD, USA). The emission intensity (AUC) was about similar for all the FGA-labeled GO nanocarriers used in this study.

The uptake of FGA-GO-CD and FGA-GO-CD-DEN by HeLa and MDA-MB-231 cells was investigated using flow cytometry. The cells (1.5×10^5 cells/well), which were seeded in 12-well culture plates and incubated for 24 h at 37 °C in a 5% CO_2 humidified chamber, were treated with FGA-GO-CD at concentrations ranging from 25 to 200 μg/ml or FGA-GO-CD-DEN at 15.6, 31.25 and 62.5 μg/ml with 2 h incubations. The treated cells were washed 2 times with cold PBS, trypsinized, transferred to tubes and centrifuged. The cells were re-

suspended in 0.5 ml of PBS containing 0.5% FBS for immediate flow cytometric analysis on a BD FACS Canto II flow cytometer (Becton Dickinson, San Jose, CA, USA) equipped with a 488 nm argon laser and a 520 nm filter to detect the fluorescence emitted by the FGA taken up by the cells. Data from 10,000 cells were collected and analyzed using FACS DIVA analysis software (Becton Dickinson).

The procedure for high-content screening was as follows: HeLa cells were incubated with FGA-GO-CD for 2 h. MDA-MB-231 cells were treated with FGA-GO, FGA-GO-CD and FGA-GO-CD-DEN for 2 h. Cells were then fixed with 4% paraformaldehyde for 15 min at 37 °C and rinsed 2 times by PBS. Then, the nucleus of each cell was stained with Hoechst 33342 (1 μg/ml) for 20 min at room temperature and rinsed with buffer. Cellular uptake of FGA-GO-CD/DOX was observed by using a Cellomic Arrayscan VTI HCS Reader (Thermo Scientific, USA). The fluorescence emission of Hoechst 33342 was measured at 461 nm under excitation at 361 nm.

3. Results and discussion

3.1. Characterization of nanocarriers

Amino-β-CD was covalently bound to 100 nm-sized GO, and DOX, an anthracycline antibiotic for the treatment of a wide range of cancer, was loaded as a model drug for chemotherapy to evaluate the loading efficiency of the nanocarrier. AFM images (Fig. 1) revealed that GO-CD nanocarrier and DOX-loaded GO-CD were morphologically globule, while GO was a flat sheet. After CD was conjugated on GO, the negative zeta potential value (−81.4 mV) of GO decreased to −52.8 mV (see Table 1), indicating that the number of carboxyl groups on GO was reduced by amidation with CD. The zeta potential of GO-CD-DEN changed with pH, with negative zeta potential value at alkaline pH and positive value at acidic pH. After DOX was loaded onto GO and GO-CD, the potentials changed from negative to positive due to the adsorption of DOX onto the GO and GO-CD. These observations indicate that DOX are loaded onto the surface of GO and GO-CD through π-π stacking, hydrophobic interaction and inclusion complexation between DOX and GO or GO-CD [7,16,26]. Moreover, protonated primary NH_2 group of DOX also contributes to potential conversion from negative to positive [1,16,26,41].

Loading of DOX on nanocarriers was examined by IR absorption spectroscopy (Table 2). The IR spectra of GO/DOX and GO-CD/DOX displayed an absorption band around 1723–1735 cm^{-1}, which is attributed to C═O stretching vibration mode and is common for GO, GO-CD, GO-CD-DEN and DOX except amino-β-CD, which has no C═O. A band around 1615–1636 cm^{-1} was observed for all the samples listed in Table 2, because they possess aromatic C═C unit in the structure. GO-CD-DEN gave two bands at 1641 cm^{-1} and 1550 cm^{-1}, attributed to amides I and II from dendrimer. The bands were strong and overlapping with the bands of OH, aromatic and NH_2 groups. A band around 1694–1701 cm^{-1} was observed for amino-β-CD, GO-CD and GO-CD/DOX, which is attributed to the OH group in CD. Meanwhile, a characteristic band at 1521–1581 cm^{-1} appeared only on DOX, GO/DOX and GO-CD/DOX but not on amino-β-CD, GO and GO-CD, suggesting NH_2 bending mode from DOX.

Loading of DOX on nanocarriers was also examined through UV–visible absorption spectroscopy (see Table 3). An absorption band at 230–245 nm of amino-β-CD, GO, GO-CD and GO-CD-DEN was overlapped by a characteristic band of DOX after loading of DOX on them. The characteristic bands of DOX at 252 and 482 nm were distinctly observed on GO/DOX, GO-CD/DOX and GO-CD-DEN/DOX, indicating the existence of DOX on the nanocarriers (GO/DOX, GO-CD/DOX and GO-CD-DEN/DOX). In addition, the red shift of the absorption band of DOX at 482 nm to a longer wavelength at 497 nm for GO/DOX and GO-CD/DOX was due to the ground-state electron donor-acceptor interaction between DOX and GO [6–8,41]. The loading of DOX on nanocarriers influenced the fluorescence emission spectra. As seen in

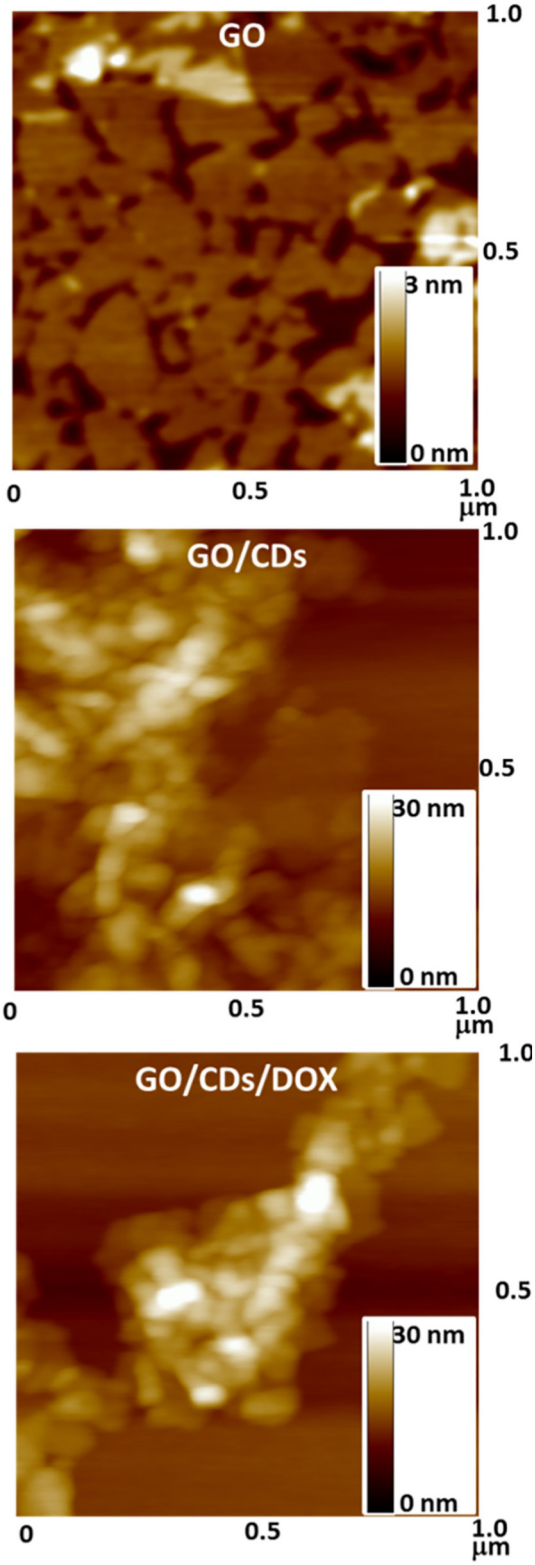

Fig. 1. AFM images of GO, GO/CDs and GO/CDs/DOX.

Table 1
Zeta potential (mV) of GO, GO-CD, GO/DOX and GO-CD/DOX.

Nanocarrier	Without DOX	With DOX
GO	−81.4	21.4
GO-CD	−52.8	49.1

Table 2
IR absorption bands (cm^{-1}) and their assignments of amino-β-CD, GO, GO-CD, DOX, GO/DOX and GO-CD/DOX.

Assignment	C=O	OH	Amide I	Aromatic	NH_2	Amide II
Amino-β-CD		1701		1627		
GO	1735			1622		
GO-CD	1735	1701		1636		
GO-CD-DEN	1720		1641			1550
DOX	1730			1616	1581	
GO/DOX	1723			1618	1521	
GO-CD/DOX	1724	1694		1615	1578	

Table 3
UV–visible absorption and fluorescence emission bands (nm) of amino-β-CD, GO, GO-CD, DOX, GO/DOX and GO-CD/DOX.

Assignment	Absorption band				Emission band		
					Excitation at 255 nm	Excitation at 480 nm	
Amino-β-CD	≃245				–		
GO	230,		sh		370		
GO-CD	240,		sh		370		
GO-CD-DEN	sh,		sh		370		
DOX	233,	252,	289,	482		560,	580
GO/DOX	230,	252,	sh,	497		560,	580
GO-CD/DOX	233,	255,	295,	497		≃560,	580

sh: shoulder.

Table 3, while amino-β-CD has no fluorescence, GO, GO-CD and GO-CD-DEN displayed an emission band at 370 nm (at 255 nm excitation). After loading of DOX, the emission bands appeared at 560 and 580 nm (at 480 nm excitation), similar to the emission band of DOX. Thus, the results from morphological observation and spectroscopic examination indicate successful loading of DOX onto the nanocarriers.

3.2. Loading and release of drugs on GO, GO-CD and GO-CD-DEN

It has been reported that the loading of DOX on GO was pH-dependent, and the DOX loading capacity was higher at neutral condition rather than at basic and acidic conditions [8,16]. Thus, in the present work, the loading of DOX on GO and GO-CD was carried out at pH 7. It initially increased with the DOX concentration and reached saturation at high DOX concentrations, as depicted in Fig. 2A. The loading amount of DOX was 1.91 and 2.27 mg/mg(carrier) at DOX concentration of 0.4 mg/ml for GO and GO-CD, respectively. The loading on GO is consistent with the previous reports that DOX loaded on GO nanosheet was 1.00 mg/mg(carrier) at a DOX concentration of 0.30 mg/ml [17] or 2.35 g/g(carrier) at 0.47 mg/ml [16], while GO possessed higher DOX loading capacity than that of polymer micelles and carbon nanotubes [1,4,42,43]. The high loading on GO might be due to the fact that DOX can be loaded on both side of the graphene sheet through π–π interaction, hydrogen bonding or electrostatic interaction [16]. Since DOX can form an inclusion complex with CD, further enhancement of the DOX loading on GO-CD, as seen in Fig. 2A, might be due to the inclusion of DOX in CD. Therefore, the introduction of CD on GO can influence on the loading capacity of GO-based nanocarriers, as DOX can be loaded on CD as well as on GO surfaces. Thus, these observations suggest that GO-CD can be utilized as a drug nanocarrier, since the drug loading capacity is higher than that of the common drug carriers such as carbon nanotubes [42], carbon nanohorns [4] and polymer micelles [1,42], which possess drug loading capacities < 1 mg/mg(carrier) at the saturated concentration of drugs [43,44].

The DOX release from GO and GO-CD was investigated at pH 5.5 and 7.4 to represent tumor environment [45] and body fluid [46], respectively. As depicted in Fig. 2B, the amount of DOX released at pH 5.5

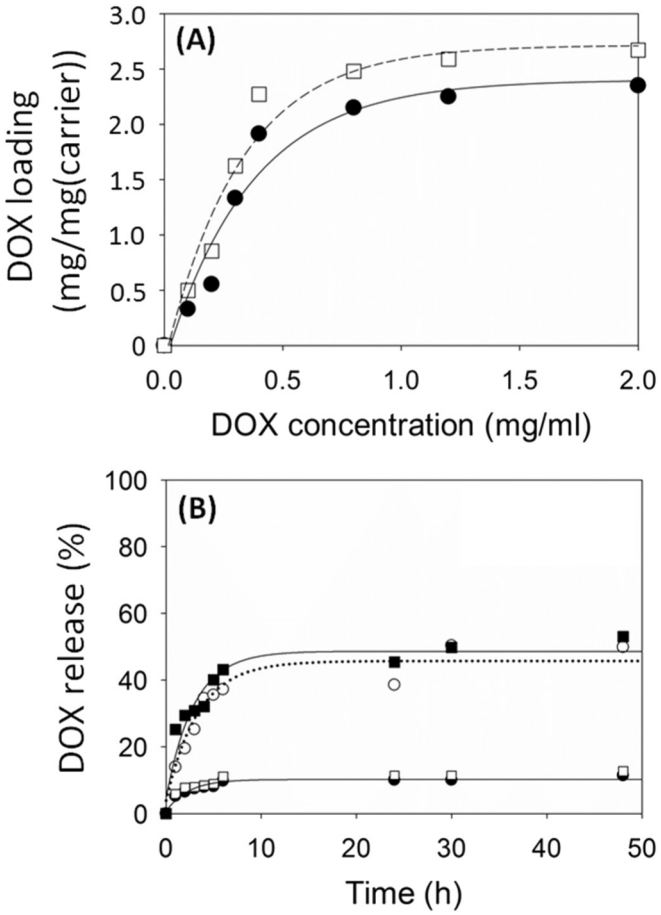

Fig. 2. (A) DOX loading on (●) GO and (□) GO-CD. (B) DOX release from (●) GO and (□) GO-CD at pH 7.4, and (○) GO and (■) GO-CD at pH 5.5.

was about 49% (0.94 mg/mg(carrier)) and 53% (1.20 mg/mg(carrier)) of the total bound DOX on GO and GO-CD, respectively. The release is lower than the 65% of DOX released from T7-modified dendrigraft poly-L-lysine with glutamic acid [46]. But, they are higher than the amount of DOX released from both GO–chitosan–FA (25%) [17] and GO–Fe_3O_4–FA (23%) [7] at pH 5.5.

Conversely, the release of DOX from GO-CD at pH 7.4 was lower, at only 10% and almost similar to that released from GO, and is consistent with previous reports that indicated 5–10% release of DOX from GO at pH 7.4 after 72 h [8,17,46]. This clearly suggests GO-DOX and GO-CD/DOX are more stable at pH 7.4, giving a lower release of DOX in the neutral condition of body fluid [45]. This could be attributed to the strong hydrogen bonding interaction between DOX and GO. At a more acidic condition in tumor environment, DOX is preferentially released from the GO or GO-CD carriers [46]. These DOX loading and release results, particularly their high drug loading capacity, imply both GO and GO-CD are potential drug nanocarriers for delivery of anticancer drugs to tumor cells.

We then further investigated the effect of an additional moiety of DEN on GO-CD by studying the loading and release profiles of DOX (chemotherapeutic), CPT (chemotherapeutic) and PpIX (photosensitizer) (Fig. 3). The loading of DOX was saturated at low drug concentration (0.4 mg DOX/mg carrier). It is about 5.7-fold lower than the drug concentration loaded on GO-CD. This was probably due to DEN conjugation interfered the adsorption of DOX on GO planar sheet. PpIX was loaded in a similar pattern to DOX but at higher saturated concentration (0.8 mg PpIX/mg carrier) than DOX. While, the loading of CPT continued to increase beyond 4 mg CPT/mg carrier. Thus, the drug loading capacity of GO-CD-DEN increased in the order: DOX <

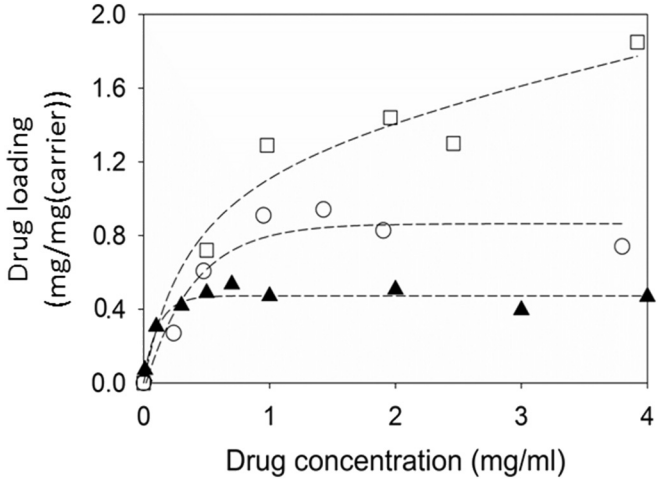

Fig. 3. Drug loading on GO-CD-DEN as a function of drug concentration. (▲) doxorubicin, (□) camptothecin, (○) protoporphyrin IX.

PpIX < CPT. These drugs loaded on GO-CD-DEN are mainly via the π-π stacking interaction with graphitic domain of GO and also through the strong hydrogen bonding interaction with GO and as inclusion in the cavity of CD on GO. The π-π stacking interaction of PpIX is expected to be stronger than DOX because of its larger planar skeleton despite not expected to form an inclusion complex in CD because of its excessively large planar structure. DOX has a bulky hydrophilic portion in addition to its quinone skeleton and PpIX has flexible alkyl acid tails. These nonplanar structures are likely to restrict the adsorption of these drugs on GO. In contrast, the completely flat π-conjugate molecular structure of CPT favors compact stacking arrangement on hydrophobic basal plane of GO resulting increased drug loading. Moreover, the hydrophobic nature of PpIX and CPT supports higher binding to the hydrophobic graphitic domain of GO compared to the more hydrophilic doxorubicin.

Fig. 4 shows drug release from drug-loaded GO-CD-DEN nanocarriers. DOX release at pH 5.5 was higher than at pH 7.4, indicating its release is pH responsive. The percentage release of CPT at pH 5.5 was similar to that of DOX, but its release at pH 7.4 was greater than that at pH 5.5. This phenomenon was probably due to the weakly acidic CPT was ionized to negatively charged carboxylate form at pH 7.4 [47], resulting in repulsion of CPT from the negatively charged GO surface, and thus had a higher percentage of release at pH 7.4. PpIX behaved differently from DOX and CPT giving a drug release of < 10%. The percentage release of PpIX from GO-CD-DEN at acidic pH was similar to that of reported in previous study [48]. The low percentage release of PpIX from GO-CD-DEN allows enhanced photocytotoxicity towards cells compared to the free PpIX as reported in the in vitro photocytotoxicity study later. The enhanced photocytotoxicity was probably due to the increased cellular uptake of PpIX delivered by GO-CD-DEN into the cells, followed by light activation of PpIX to create reactive oxygen species that killed cells effectively.

3.3. In vitro cytotoxicity and photocytotoxicity of GO-based nanocarriers

The cell viability following treatment of GO-CD/DOX and free DOX was determined after 72 h incubation using the MTT assay in MDA-MB-231 cells and HeLa cells. As a control, GO and GO-CD nanocarriers showed minimal toxicity in HeLa cells with an IC_{50} of 86 and 72 μg/ml, respectively. These values are approximately 10-fold higher than those of GO-CD/DOX (Table 4). Similar observation was found in MDA-MD-231 cells where the IC_{50} of GO was higher than 100 μg/ml and the IC_{50} of GO-CD was approximately 40 times higher than GO-CD/DOX (Table 4). These indicate that the observed cytotoxicity of GO-CD/DOX is resulting from the DOX loaded on GO-CD nanocarrier instead of the drug carrier itself.

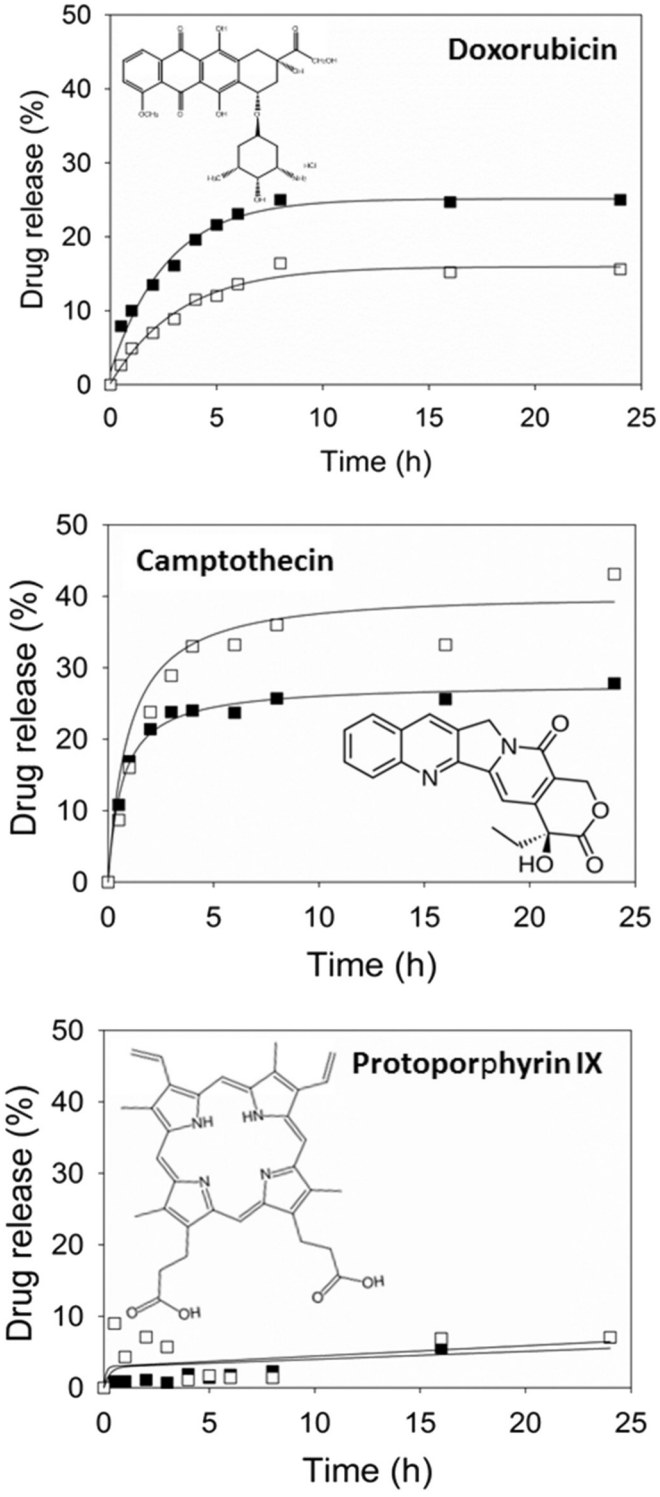

Fig. 4. Drug release of doxorubicin, camptothecin, protoporphyrin IX from GO-CD-DEN/drug. (□) pH 7.4, (■) pH 5.5.

The GO-CD/DOX demonstrated enhanced cytotoxicity in MDA-MB-231 breast cancer cells, with an IC_{50} of 0.3 μg/ml DOX equivalent compared to free DOX (IC_{50} = 3.3 μg/ml) under identical conditions (Table 4). Conversely, GO-CD/DOX exhibited approximately 6-fold less cytotoxicity compared to free DOX in HeLa cervical cancer cells. This implies that GO-CD/DOX has a better cytotoxicity profile in MDA-MB-231 breast cancer cells.

Table 4
IC_{50} values of GO, GO-CD, DOX and GO-CD/DOX in HeLa and MDA-MB-231 cells.

Samples	IC_{50} (μg/ml)	
	HeLa	MDA-MB-231
GO	86	> 100
GO-CD	72	12.5
DOX	1.2	3.3
GO-CD/DOX	7.5	0.3

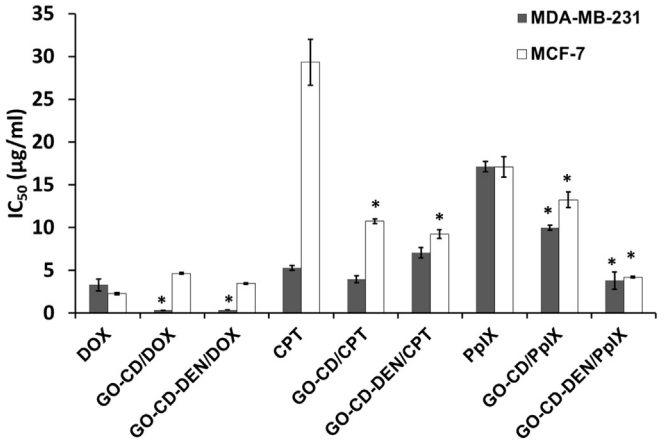

Fig. 5. IC_{50} values of GO-CD-DEN/drugs, GO-CD/drugs and free drugs. Data are expressed as mean ± SEM (n = 3). *$p < 0.05$ compared to free drug, One-Way ANOVA.

From here, we further investigated the potential of GO-CD and GO-CD-DEN as delivery carriers for different classes of anticancer drugs including DOX and CPT, which are chemotherapeutics, and PpIX, which is a photosensitizer, in breast cancer models (Fig. 5). In our previous work, we demonstrated that functionalization of GO with dendrimers was able to improve water solubility and increase the uptake of the nanocarriers in cancer cells [38]. Therefore, GO-CD-DEN nanocarriers loaded with different drugs were prepared and their in vitro cytotoxicity in MDA-MB-231 and MCF-7 breast cancer cells were evaluated.

In MDA-MB-231 cells, both GO-CD/DOX and GO-CD-DEN/DOX showed enhanced cytotoxicity (IC_{50} = 0.3 μg/ml) when comparing with free DOX (IC_{50} = 3.3 μg/ml). In the case of CPT, no significant difference ($p > 0.05$, One-Way ANOVA) among GO-CD/CPT, GO-CD-DEN/CPT and free CPT was observed. However, GO-CD-DEN had significantly increased the photocytotoxicity of PpIX (IC_{50} = 0.3 μg/ml) by 3- and 4-fold compared to GO-CD/PpIX and free PpIX, respectively (Fig. 5).

In MCF-7 cells, DOX, CPT and PpIX loaded on GO-CD-DEN showed better cytotoxicity when compared to those loaded on GO-CD. The IC_{50} of DOX, CPT and PpIX was 1.3-, 1.2- and 3-fold lower when loaded in GO-CD-DEN than those loaded in GO-CD. The GO-CD-DEN/CPT and GO-CD-DEN/PpIX also showed better efficacy compared to free CPT and PpIX with lower IC_{50} by 3- and 4-fold, respectively. Conversely, no significant difference was observed between GO-CD-DEN/DOX and free DOX (Fig. 5).

These findings show that GO-CD and GO-CD-DEN improved the cytotoxicity of DOX in MDA-MB-231 and CPT in MCF-7 cancer cells. They also enhanced the photocytotoxicity of PpIX in both cancer cells. These indicate that GO-CD and GO-CD-DEN are potential delivery agents for selected chemotherapeutics and photosensitizers in cancer therapy.

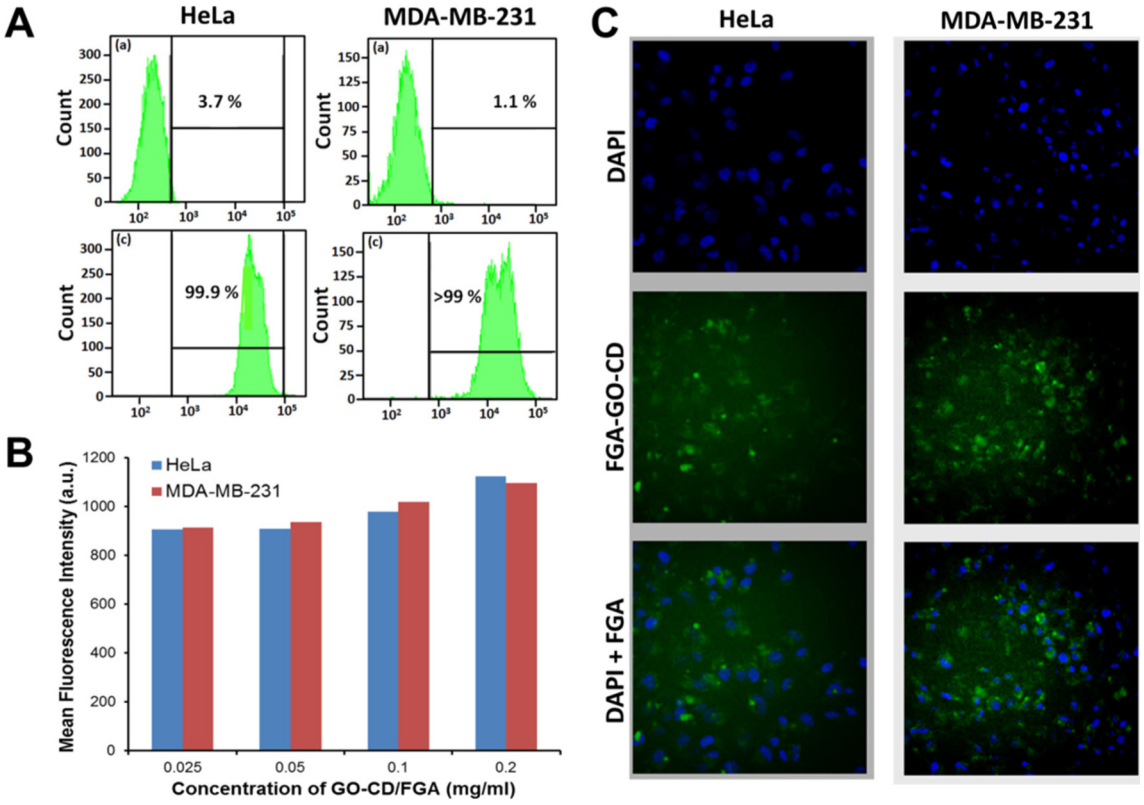

Fig. 6. Cellular uptake of FGA-GO-CD in HeLa and MDA-MB-231 cells using flow cytometry and high content screening. (A) Percentage of cellular uptake of FGA-GO-CD at 62.5 μg/ml in cancer cells at 2 h of incubation. Upper panel: without FGA-GO-CD treatment; Lower panel: treated with FGA-GO-CD. (B) FGA-GO-CD concentration dependence of cellular uptake expressed in mean fluorescence intensity at 2 h of incubation. (C) High content screening images of FGA-GO-CD on DAPI-labeled cells at 62.5 μg/ml at 2 h of incubation. (For interpretation of the references to color in this figure, the reader is referred to the web version of this article.)

3.4. Cellular uptake of FGA-labeled GO nanocarriers by flow cytometry and high content screening

Cellular uptake of FGA-GO-CD and FGA-GO-CD-DEN by HeLa and MDA-MB-231 cancer cells was determined using flow cytometry based on the fluorescence of FGA conjugated to the nanohybrids. FGA-GO-CD exhibited the highest uptake of > 99.9% after incubation for 2 h in both HeLa and MDA-MB-231 cells (Fig. 6A). The mean fluorescence intensities showed that the cellular uptake of FGA-GO-CD increased in a concentration dependent manner from 0.025–0.2 mg/ml. The uptake amount was similar between HeLa and MDA-MB-231 cells (Fig. 6B).

The cellular uptake of the FGA-GO-CD was also examined using high content screening based on the green fluorescence of FGA after 2 h incubation in HeLa and MDA-MB-231 cells (Fig. 6C). High intensities of green fluorescence of FGA were observed in both cancer cell lines, mostly in the cytoplasm (Fig. 6C). There was no overlapping of green fluorescence of FGA and blue fluorescence of DAPI that stains the cell nuclei. This indicates that the nanohybrids remained in the cytoplasm and did not enter the nucleus.

For FGA-GO-CD-DEN, the cellular uptake in MDA-MD-231 cells was increased in a concentration dependent manner. The uptake of FGA-GO-CD-DEN was 47.5, 90.6 and 99.4% when incubated MDA-MB-231 cells with 15.6, 31.25 and 62.5 μg/ml of nanocarriers for 2 h (Fig. 7A). In high content screening, the FGA-labeled GO-CD and GO-CD-DEN exhibited higher intensities of green fluorescence compared to FGA-labeled GO (Fig. 7B). The green fluorescence of FGA in GO, GO-CD and GO-CD-DEN also did not co-localized with the blue fluorescence from DAPI in the nucleus. These results indicate that functionalization of GO with CD and CD-DEN had increased the uptake of nanocarriers in cancer cells. Similar to FGA-GO-CD, the uptaken FGA-GO-CD-DEN also did not enter the nucleus but localized mainly in the cytoplasm. In addition, the higher uptake of GO-CD and GO-CD-DEN also resulted in higher cytotoxicity in cancer cells when they are loaded with various anticancer drugs including DOX, CPT and PpIX as discussed earlier (Fig. 5).

4. Conclusions

In conclusion, this study shows that GO-CD and GO-CD-DEN are potential nanocarriers for anticancer drugs including chemotherapeutics and photosensitizers. In addition to their high drug loading capacity, GO-CD and GO-CD-DEN was able to enhance the cytotoxicity of chemotherapeutics including DOX and CPT, and also the photocytotoxicity of PpIX by increasing the uptake of the GO-CD-drug and GO-CD-DEN-drug nanohybrids in cancer cells. Further conjugation with targeted ligands may give the drug-loaded GO-nanohybrids active

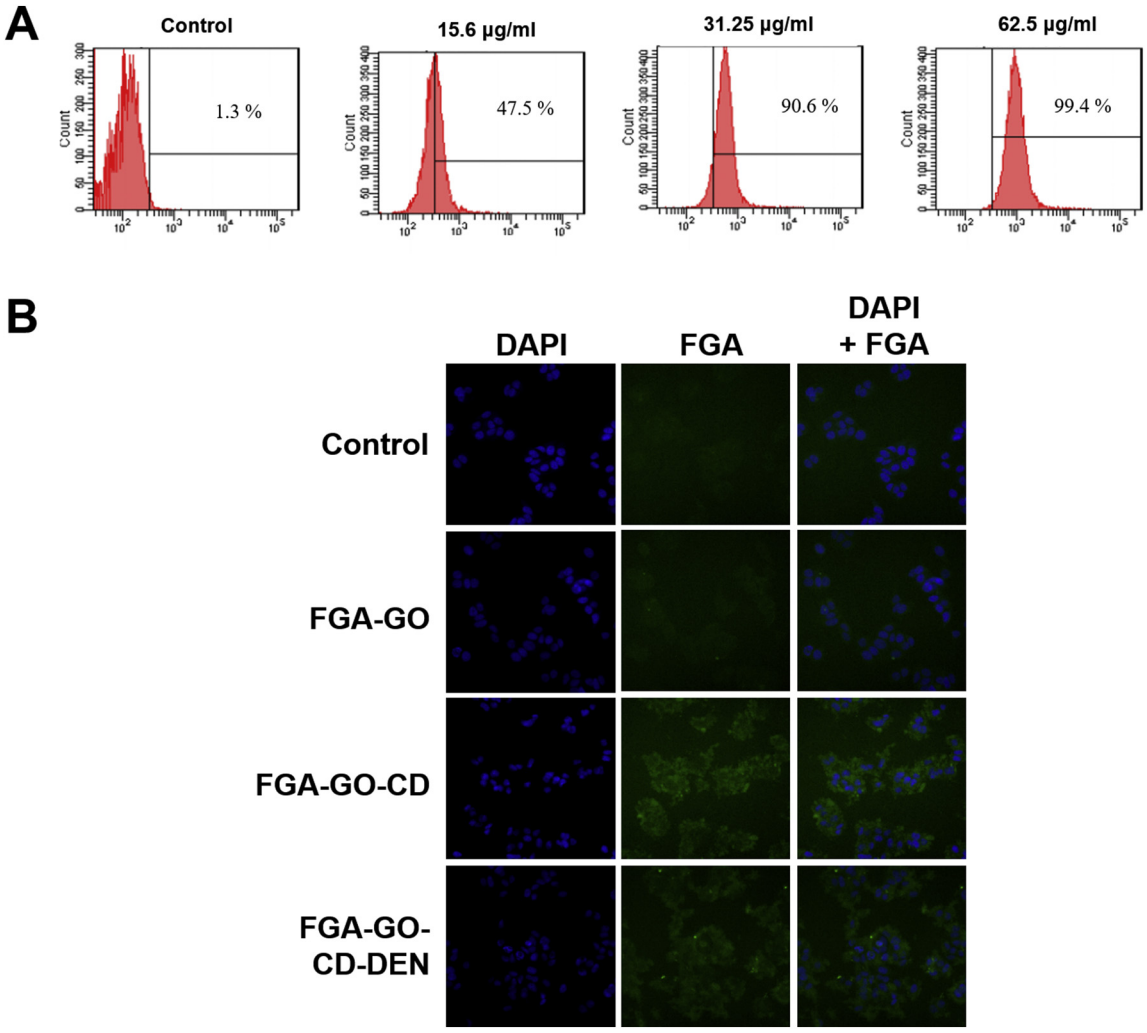

Fig. 7. Cellular uptake of FGA-GO-CD-DEN in MDA-MB-231 cells using flow cytometry and high content screening. (A) Percentage of cellular uptake of FGA-GO-CD-DEN (15.6, 31.25 and 62.5 μg/ml) in MDA-MB-231 cells at 2 h of incubation. (B) High content screening images of FGA-GO, FGA-GO-CD and FGA-GO-CD-DEN on DAPI-labeled cells at 62.5 μg/ml at 2 h of incubation. (For interpretation of the references to color in this figure, the reader is referred to the web version of this article.)

targeting properties to further improve tumor selectivity of anticancer drugs for chemotherapy and photodynamic therapy.

Conflict of interest

We have no conflict of interest to declare.

Acknowledgements

This study was carried out under bilateral cooperation programs between the National Taiwan University of Science and Technology of Taiwan and the University of Malaya of Malaysia, and was supported financially by the Ministry of Higher Education, Malaysia's HIR-MOHE grants (UM.C/625/1/HIR/MOHE/MED/17 and UM.C/625/1/HIR/MOHE/MED/33). AS gratefully acknowledges National Science Council, Taiwan, for Postdoctoral Fellowship (NSC 102-2221-E-011-114).

References

[1] Z. Liu, X. Sun, N. Nakayama-Ratchford, H. Dai, Supramolecular chemistry on water-soluble carbon nanotubes for drug loading and delivery, ACS Nano 1 (2007) 50–56.
[2] J. Chen, S. Chen, X. Zhao, L.V. Kuznetsova, S.S. Wong, I. Ojima, Functionalized single-walled carbon nanotubes as rationally designed vehicles for tumor-targeted drug delivery, J. Am. Chem. Soc. 130 (2008) 16778–16785.
[3] A.A. Bhirde, V. Patel, J. Gavard, G. Zhang, A.A. Sousa, A. Masedunskas, R.D. Leapman, R. Weigert, J.S. Gutkind, J.F. Rusling, Targeted killing of cancer cells in vivo and in vitro with EGF-directed carbon nanotube-based drug delivery, ACS Nano 3 (2009) 307–316.
[4] T. Murakami, K. Ajima, J. Miyawaki, M. Yudasaka, S. Iijima, K. Shiba, Drug-loaded carbon nanohorns: adsorption and release of dexamethasone in vitro, Mol. Pharm. 1 (2004) 399–405.
[5] J. Xu, M. Yudasaka, S. Kouraba, M. Sekido, Y. Yamamoto, S. Iijima, Single wall carbon nanohorn as a drug carrier for controlled release, Chem. Phys. Lett. 461 (2008) 189–192.
[6] L. Zhang, J. Xia, Q. Zhao, L. Liu, Z. Zhang, Functional graphene oxide as a nanocarrier for controlled loading and targeted delivery of mixed anticancer drugs, Small 6 (2010) 537–544.
[7] Y. Yang, Y.M. Zhang, Y. Chen, D. Zhao, J.T. Chen, Y. Liu, Construction of a graphene oxide based noncovalent multiple nanosupramolecular assembly as a scaffold for drug delivery, Chemistry 18 (2012) 4208–4215.
[8] X. Yang, Y. Wang, X. Huang, Y. Ma, Y. Huang, R. Yang, H. Duan, Y. Chen, Multi-functionalized graphene oxide based anticancer drug-carrier with dual-targeting function and pH-sensitivity, J. Mater. Chem. 21 (2011) 3448–3454.
[9] D. Kai, S.S. Liow, X.J. Loh, Biodegradable polymers for electrospinning: towards biomedical applications, Mater. Sci. Eng. C 45 (2014) 659–670.
[10] Q.Q. Dou, S.S. Liow, E. Ye, R. Lakshminarayanan, X.J. Loh, Biodegradable thermogelling polymers: working towards clinical applications, Adv. Healthc. Mater. 3 (2014) 977–988.
[11] X.J. Loh, J. Li, Biodegradable thermosensitive copolymer hydrogels for drug delivery, Expert Opin. Ther. Pat. 17 (2007) 965–977.
[12] Z. Li, E. Ye, David, R. Lakshminarayanan, X.J. Loh, Recent advances of using hybrid nanocarriers in remotely controlled therapeutic delivery, Small 12 (2016) 4782–4806.
[13] X.J. Loh, S.J. Ong, Y.T. Tung, H.T. Choo, Co-delivery of drug and DNA from cationic dual-responsive micelles derived from poly(DMAEMA-co-PPGMA), Mater. Sci. Eng. C 33 (2013) 4545–4550.
[14] S.S. Liow, Q. Dou, D. Kai, Z. Li, S. Sugiarto, C.Y.Y. Yu, R.T.K. Kwok, X. Chen, Y.-L. Wu, S.T. Ong, A. Kizhakeyil, N.K. Verma, B.Z. Tang, X.J. Loh, Long-term real-time in vivo drug release monitoring with AIE thermogelling polymer, Small 13 (2017) 1603404.
[15] X.T. Zheng, C.M. Li, Restoring basal planes of graphene oxides for highly efficient loading and delivery of beta-lapachone, Mol. Pharm. 9 (2012) 615–621.
[16] X. Yang, X. Zhang, Z. Liu, Y. Ma, Y. Huang, Y. Chen, High-efficiency loading and controlled release of doxorubicin hydrochloride on graphene oxide, J. Phys. Chem. C 112 (2008) 17554–17558.
[17] D. Depan, J. Shah, R.D.K. Misra, Controlled release of drug from folate-decorated and graphene mediated drug delivery system: synthesis, loading efficiency, and drug release response, Mater. Sci. Eng. C 31 (2011) 1305–1312.
[18] J. Kim, L.J. Cote, F. Kim, W. Yuan, K.R. Shull, J. Huang, Graphene oxide sheets at interfaces, J. Am. Chem. Soc. 132 (2010) 8180–8186.
[19] Z. Liu, J.T. Robinson, X. Sun, H. Dai, PEGylated nanographene oxide for delivery of water-insoluble cancer drugs, J. Am. Chem. Soc. 130 (2008) 10876–10877.
[20] M.E. Brewster, T. Loftsson, Cyclodextrins as pharmaceutical solubilizers, Adv. Drug Deliv. Rev. 59 (2007) 645–666.
[21] J. Li, X.J. Loh, Cyclodextrin-based supramolecular architectures: syntheses, structures, and applications for drug and gene delivery, Adv. Drug Deliv. Rev. 60 (2008) 1000–1017.
[22] A. Harada, Cyclodextrin-based molecular machines, Acc. Chem. Res. 34 (2001) 456–464.
[23] H. Ye, C. Owh, S. Jiang, C. Ng, D. Wirawan, X. Loh, A thixotropic polyglycerol sebacate-based supramolecular hydrogel as an injectable drug delivery matrix, Polym. 8 (2016) 130.
[24] G. Barouti, S.S. Liow, Q. Dou, H. Ye, C. Orione, S.M. Guillaume, X.J. Loh, New linear and star-shaped thermogelling poly ([R]-3-hydroxybutyrate) copolymers, Chem. Eur. J. 22 (2016) 10501–10512.
[25] Z. Li, X.J. Loh, Water soluble polyhydroxyalkanoates: future materials for therapeutic applications, Chem. Soc. Rev. 44 (2015) 2865–2879.
[26] O. Bekers, J.J. Van Den Bosch Kettenes, S.P. Van Helden, D. Seijkens, J.H. Beijnen, A. Bulti, W.J.M. Underberg, Inclusion complex formation of anthracycline antibiotics with cyclodextrins; a proton nuclear magnetic resonance and molecular modelling study, J. Incl. Phenom. Mol. Recognit. Chem. 11 (1991) 185–193.
[27] O. Swiech, A. Mieczkowska, K. Chmurski, R. Bilewicz, Intermolecular interactions between doxorubicin and β-cyclodextrin 4-methoxyphenol conjugates, J. Phys. Chem. B 116 (2012) 1765–1771.
[28] O. Bekers, J.H. Beijnen, M. Otagiri, A. Bult, W.J.M. Underberg, Inclusion complexation of doxorubicin and daunorubicin with cyclodextrins, J. Pharm. Biomed. Anal. 8 (1990) 671–674.
[29] J. Pushpamalar, A.K. Veeramachineni, C. Owh, X.J. Loh, Biodegradable polysaccharides for controlled drug delivery, ChemPlusChem 81 (2016) 504–514.
[30] H. Ye, A.A. Karim, X.J. Loh, Current treatment options and drug delivery systems as potential therapeutic agents for ovarian cancer: a review, Mater. Sci. Eng. C 45 (2014) 609–619.
[31] Y. Xiang, N.N.L. Oo, J.P. Lee, Z. Li, X.J. Loh, Recent development of synthetic nonviral systems for sustained gene delivery, Drug Discov. Today (2017), http://dx.doi.org/10.1016/j.drudis.2017.04.001.
[32] T. Nakanishi, S. Fukushima, K. Okamoto, M. Suzuki, Y. Matsumura, M. Yokoyama, T. Okano, Y. Sakurai, K. Kataoka, Development of the polymer micelle carrier system for doxorubicin, J. Control. Release 74 (2001) 295–302.
[33] X.J. Loh, T.-C. Lee, Q. Dou, G.R. Deen, Utilising inorganic nanocarriers for gene delivery, Biomater. Sci. 4 (2016) 70–86.
[34] R. Duncan, L. Izzo, Dendrimer biocompatibility and toxicity, Adv. Drug Deliv. Rev. 57 (2005) 2215–2237.
[35] S.H. Medina, M.E.H. El-Sayed, Dendrimers as carriers for delivery of chemotherapeutic agents, Chem. Rev. 109 (2009) 3141–3157.
[36] X. Li, T. Imae, D. Leisner, M.A. López-Quintela, Lamellar structures of anionic poly (amido amine) dendrimers with oppositely charged didodecyldimethylammonium bromide, J. Phys. Chem. B 106 (2002) 12170–12177.
[37] V. Tiriveedhi, K.M. Kitchens, K.J. Nevels, H. Ghandehari, P. Butko, Kinetic analysis of the interaction between poly(amidoamine) dendrimers and model lipid membranes, Biochim. Biophys. Acta Biomembr. 1808 (2011) 209–218.
[38] A. Siriviriyanun, M. Popova, T. Imae, L.V. Kiew, C.Y. Looi, W.F. Wong, H.B. Lee, L.Y. Chung, Preparation of graphene oxide/dendrimer hybrid carriers for delivery of doxorubicin, Chem. Eng. J. 281 (2015) 771–781.
[39] J. Szejtli, Introduction and general overview of cyclodextrin chemistry, Chem. Rev. 98 (1998) 1743–1754.
[40] C.F. Potter, N.R. Russell, M. McNamara, Spectroscopic characterisation of metallocyclodextrins for potential chiral separation of amino acids and L/D-DOPA, J. Incl. Phenom. Macrocycl. Chem. 56 (2006) 395–403.
[41] J.M. Schuette, T. Ndou, A. Munoz de la Pena, K.L. Greene, C.K. Williamson, I.M. Warner, Characterization of the .beta.-cyclodextrin/acridine complex, J. Phys. Chem. 95 (1991) 4897–4902.
[42] H. Hu, J. Yu, Y. Li, J. Zhao, H. Dong, J. Biomed. Mater. Res. A 100 (2012) 141–148.
[43] C. Yang, J.P.K. Tan, W. Cheng, A.B.E. Attia, C.T.Y. Ting, A. Nelson, J.L. Hedrick, Y.-Y. Yang, Supramolecular nanostructures designed for high cargo loading capacity and kinetic stability, Nano Today 5 (2010) 515–523.
[44] K.K. Karukstis, E.H.Z. Thompson, J.A. Whiles, R.J. Rosenfeld, Deciphering the fluorescence signature of daunomycin and doxorubicin, Biophys. Chem. 73 (1998) 249–263.
[45] Q. Sun, S. Cai, B.R. Peterson, Selective disruption of early/recycling endosomes: release of disulfide-linked cargo mediated by a N-alkyl-3β-cholesterylamine-capped peptide, J. Am. Chem. Soc. 130 (2008) 10064–10065.
[46] S. Liu, Y. Guo, R. Huang, J. Li, S. Huang, Y. Kuang, L. Han, C. Jiang, Gene and doxorubicin co-delivery system for targeting therapy of glioma, Biomaterials 33 (2012) 4907–4916.
[47] D.J. Adams, L.R. Morgan, Tumor physiology and charge dynamics of anticancer drugs: implications for camptothecin-based drug development, Curr. Med. Chem. 18 (2011) 1367–1372.
[48] F. Li, S.-J. Park, D. Ling, W. Park, J.Y. Han, K. Na, K. Char, Hyaluronic acid-conjugated graphene oxide/photosensitizer nanohybrids for cancer targeted photodynamic therapy, J. Mater. Chem. B 1 (2013) 1678–1686.